Journal of Alloys and Compounds 480 (2009) 5–8

Contents lists available at ScienceDirect

Journal of Alloys and Compounds

journal homepage: www.elsevier.com/locate/jallcom

Hydrogen storage in Ti–Mn–(FeV) BCC alloys

S.F. Santos*, J. Huot

IRH - Université du Québec à Trois-Rivières, 3351 Boul. des Forges, G9A5H7 Canada

ARTICLE INFO

Article history:
Received 16 July 2008
Received in revised form
30 September 2008
Accepted 30 September 2008
Available online 20 November 2008

PACS:
68.43.−h
74.70.Ad
61.05.cp
61.66.Bi

Keywords:
Hydrogen absorbing materials
Metal hydrides

ABSTRACT

Recently, the replacement of vanadium by the less expensive (FeV) commercial alloy has been investigated in Ti–Cr–V BCC solid solutions and promising results were reported. In the present work, this approach of using (FeV) alloys is adopted to synthesize alloys of the Ti–Mn–V system. Compared to the V-containing alloys, the alloys containing (FeV) have a smaller hydrogen storage capacity but a larger reversible hydrogen storage capacity, which is caused by the increase of the plateau pressure of desorption. Correlations between the structure and the hydrogen storage properties of the alloys are also discussed.

© 2008 Elsevier B.V. All rights reserved.

1. Introduction

Environmental and economical problems associated with the consumption of fossil fuels have motivated the search for renewable and environmental friendly sources of energy. In this scenario, hydrogen emerges as an ideal energy carrier due to its large chemical energy per mass, availability, and environmental safety [1]. However, the large-scale utilization of hydrogen as energy carrier has been hindered by a number of economical and technological problems that must be conveniently solved. A key technological challenge to be overcome is the form of storing hydrogen which is a very important issue for the transport sector [2].

Because of their compactness and safety, metal hydrides are considered to be one of the most convenient ways of storing hydrogen. However, the hydrides which are operational near ambient temperature have low hydrogen storage capacities while hydrides with large capacities such as MgH_2 (7.6 wt.% H) have a high temperature of operation.

Taking the abovementioned into account, the Ti–V-based body-centered cubic (BCC) solid solutions have attracted attention for hydrogen storage applications due to their larger gravimetric storage capacities than the conventional AB_5 type alloys and the more suitable operational temperatures than those of the high capacity hydrides, such as MgH_2. The hydrogen reaction kinetics of the Ti–V binary alloys is slow and improvements are obtained by adding a third element. The first reports on Ti–V–TM (TM = transition metal) alloys were done by Maeland et al. [3] who investigated the effect of Fe, Mn, Co, Cr, and Ni on the hydrogenation reaction kinetics and observed that all investigated third elements enhanced the reaction rate.

In Ti–V alloys, the reversible hydrogen storage capacity of the BCC solid solutions is smaller than the total hydrogen storage capacity. This behavior is due to the two steps of hydrogenation in these alloys, i.e., two plateau pressures in the pressure-composition isotherms (PCI). The first plateau appears at low pressure, forming a mono-hydride, while the second one appears at higher pressure and is due to the transformation of the mono-hydride into a di-hydride. Usually, only the di-hydride contributes to the reversible hydrogen storage capacity since the mono-hydride is too stable to release hydrogen at reasonable temperature [4].

Iba and Akiba [5] investigated Ti–V–Mn multiphase ternary alloys and reported that BCC solid solutions containing precipitates of C14 Laves phases presented better reversible hydrogen sorption properties than those of single-phase BCC solid solutions. These multiphase alloys were named *Laves phase related BCC solid solutions* [6].

* Corresponding author. Present address: Institute of Chemistry of São Carlos, University of São Paulo, Av. Trab. São-carlense 400, C.P. 780, CEP 13560-970, São Carlos, SP, Brazil. Tel.: +55 16 33738042; fax: +55 16 33739903.
E-mail address: sfsantos91@yahoo.com.br (S.F. Santos).

0925-8388/$ – see front matter © 2008 Elsevier B.V. All rights reserved.
doi:10.1016/j.jallcom.2008.09.191

The Ti–V-based BCC solid solutions with better reversible hydrogen storage capacities usually have comparable high vanadium contents. From an economical point of view, the minimization of the vanadium content is mandatory since it is a very expensive raw material. However, the replacement of vanadium is a difficult task since its presence is important to ensure high hydrogen-absorbing capacities and also to stabilize the BCC structure of some Ti alloys at room temperature. Recently, the replacement of pure vanadium by a less expensive (FeV) commercial alloy has been investigated in the Ti–Cr–V system [7–10]. Taizhong et al. [7] investigated the $TiCr_{1.8-x}(FeV)_x$ alloy series, obtaining the best results of hydrogen storage for the $TiCr_{1.2}(FeV)_{0.6}$ alloy, composed of a C14 Laves phase dispersed in a BCC solid solution. This alloy showed 3.0 wt.% of total hydrogen storage capacity and 1.8 wt.% of reversible hydrogen storage capacity at 303 K in a pressure range of 10^{-4} to 3.0 MPa. The same group also reported good hydriding properties for the $TiCr(FeV)_{0.5}$ alloy, which reached 3.5 wt.% of total hydrogen storage capacity and 1.8 wt.% of reversible hydrogen storage capacity [9]. Santos and Huot [10] investigated the $TiCr_{1.2}(FeV)_x$ alloys ($x = 0.6$, 0.5, and 0.4) and obtained the best hydrogen sorption properties for the multiphase $TiCr_{1.2}(FeV)_{0.4}$ alloys, which corresponded to a total hydrogen storage capacity and reversible hydrogen storage capacity of 2.8 and 1.4 wt.%, respectively.

In the present work, this approach of replacing V by a (FeV) alloy in Ti–V–Mn BCC solid solutions is adopted. To analyze the effect of (FeV) in this alloy system, two Ti–Mn–V alloys with compositions $TiMn_{1.1}V_{0.9}$ and $TiMn_{0.9}V_{1.1}$ were synthesized and had their structures and hydrogen sorption properties compared with the $TiMn_{1.1}(FeV)_{0.9}$ and $TiMn_{0.9}(FeV)_{1.1}$ alloys similarly synthesized.

2. Experimental

The alloys were synthesized by arc melting, starting from Ti, Mn, and V elements (purity > 99%) and a (FeV) commercial alloy as raw materials. The chemical composition of this (FeV) alloy used as raw material, measured with an Oxford - Link 300 energy dispersive spectroscope (EDS), was (in at.%): 79.88 of V; 16.26 of Fe; 3.74 of Al; 0.09 of Si; 0.03 of Cr.

The arc melting was carried out under an argon atmosphere and each sample was remelted at least three times to ensure a good homogeneity of the ingot.

The structural characterization of the alloys was carried out by X-ray diffraction (XRD) using a Rigaku D-max diffractometer with Cu Kα radiation. The microstructures were analyzed by scanning electron microscopy (SEM) using a Philips XL30 microscope equipped with a backscattered electrons detector.

The hydrogen sorption properties of the as-cast samples were measured with a computer-controlled Sieverts-type apparatus. The activation was carried out at a constant hydrogen pressure of 2.0 MPa and 298 K and dehydrogenation was done at 0.030 MPa and the same temperature. Prior to the PCI measurements, the samples were fully dehydrogenated by maintaining them under vacuum for 14 h at 473 K. The PCI measurements were carried out at 353 K up to a pressure of 2.0 MPa.

3. Results and discussion

Fig. 1 shows the XRD patterns of the investigated alloys. The three most intense peaks (x) in the diffraction patterns belong to the BCC solid solution. For the $TiMn_{0.9}V_{1.1}$ alloy, the structure was almost single-phase BCC solid solution, but some small peaks of the C14 Laves phase can still be detected. This agrees with the results of Mouri and Iba [11] who reported that the $TiMn_{0.9}V_{1.1}$ alloy synthesized by arc-melting presented composition of 96.1 wt.% of BCC solid solution and 3.9 wt.% of C14 Laves phase. Decreasing of the V content in the alloys leads to the increase in intensity of the C14 diffraction peaks, as can be observed comparing the patterns of the $TiMn_{1.1}V_{0.9}$ and $TiMn_{0.9}V_{1.1}$ alloys (Fig. 1). Mouri and Iba [11] also observed that increasing the amount of vanadium in Ti–Mn–V alloys, the amount of BCC phase increases.

Replacing vanadium by ferrovanadium in the alloys leads to an increase in the relative intensity of the diffraction peaks of C14 Laves phase. The (FeV)-containing alloys also showed a contraction of the

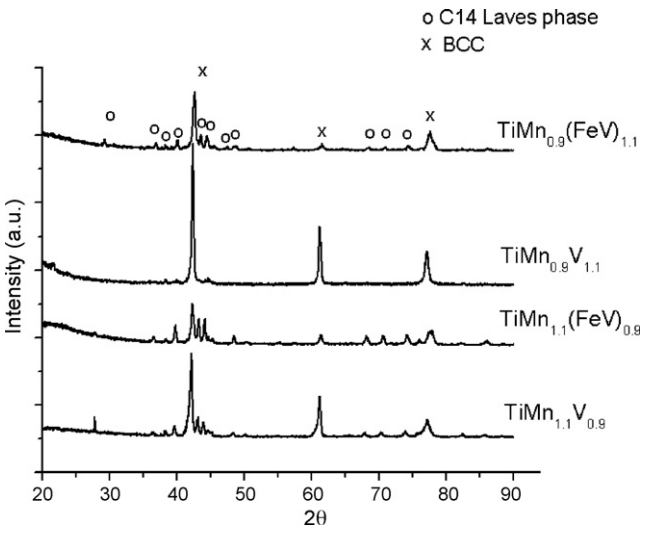

Fig. 1. XRD patterns of the Ti–Mn–V and Ti–Mn–(FeV) alloys.

cell volume of BCC phase (Table 1), probably caused by the smaller atomic radius of iron compared to that of vanadium. Challet et al. [12] observed that the increase in Fe content resulted in a decrease of the cell volume in Ti–V–Fe BCC solid solution.

Fig. 2 shows the change of microstructure upon replacement of vanadium by ferrovanadium. For the $TiMn_{0.9}V_{1.1}$ alloy, the micrograph (a) shows a nearly single-phase structure (BCC phase) with some small C14 particles in the BCC matrix. For the $TiMn_{0.9}(FeV)_{1.1}$, the micrograph (b) shows a clear two-phase microstructure consisting of BCC and C14 Laves phases. These results agree with the diffraction patterns shown in Fig. 1. The microstructures of $TiMn_{1.1}V_{0.9}$ and $TiMn_{1.1}(FeV)_{0.9}$ alloys are shown in Fig. 3a and b, respectively. For the $TiMn_{1.1}V_{0.9}$, the two-phase structure identified in the diffraction pattern of Fig. 1 is clearly seen. The replacement of vanadium by ferrovanadium resulted in the growth of the C14 colonies and an increased amount of this phase.

EDS of the investigated alloys indicated that the light phase in the alloys is richer in vanadium than the dark one. On the other hand, the dark phase is richer in Ti, Mn and Fe than the light one. These results indicate that the light phase is the BCC solid solution while the dark one is a Laves phase because it is expectable to have larger contents of V in the BCC phase and larger contents of Fe and Ti in the Laves phase [13].

Fig. 4 shows the hydrogen activation curves for the Ti–Mn–V and Ti–Mn–(FeV) alloys at 298 K. The (FeV)-containing alloys exhibited faster activation than the V-containing alloys. In the case of $TiMn_{0.9}V_{1.1}$ alloy, the activation is very slow up to about 1500 s and than proceeds at a faster rate. This incubation time is most probably due to the fact that this alloy is almost single-phase BCC. When vanadium is replaced by ferrovanadium, the two-phase (C14 + BCC) $TiMn_{0.9}(FeV)_{1.1}$ alloy almost immediately absorb hydrogen at a fast rate. The improvement is less drastic with the $TiMn_{1.1}V_{0.9}$ and $TiMn_{1.1}(FeV)_{0.9}$ alloys because the alloy containing pure vanadium

Table 1
Lattice constants and cell volumes of the BCC phases in Ti–Mn–V and Ti–Mn–(FeV) alloys. Uncertainties are estimated to be 0.0002 Å for the lattice parameters and 0.0008 Å for the cell volumes.

Alloys	Lattice parameter (Å)	Cell volume (Å^3)
$TiMn_{0.9}(FeV)_{1.1}$	3.0188	27.511
$TiMn_{0.9}V_{1.1}$	3.0240	27.655
$TiMn_{1.1}(FeV)_{0.9}$	3.0165	27.449
$TiMn_{1.1}V_{0.9}$	3.0286	27.779

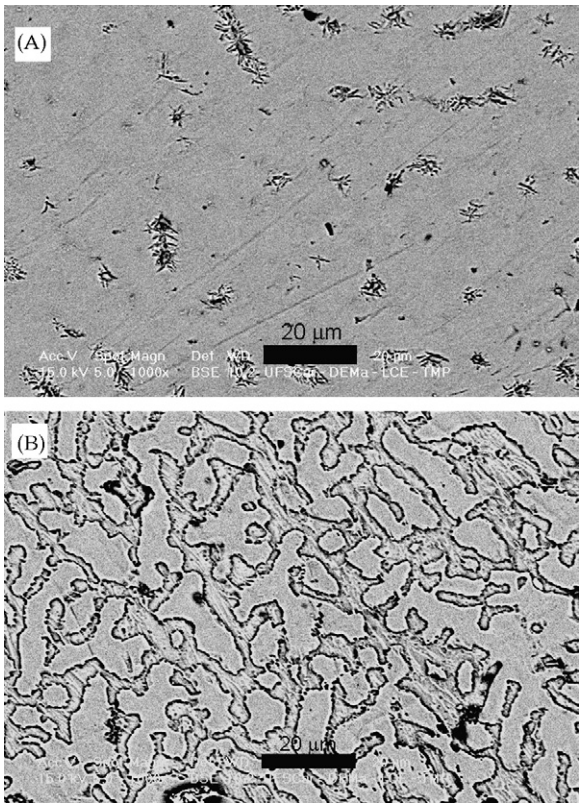

Fig. 2. (a) BSE image of the $TiMn_{0.9}V_{1.1}$ alloy and (b) BSE image of the $TiMn_{0.9}(FeV)_{1.1}$ alloy.

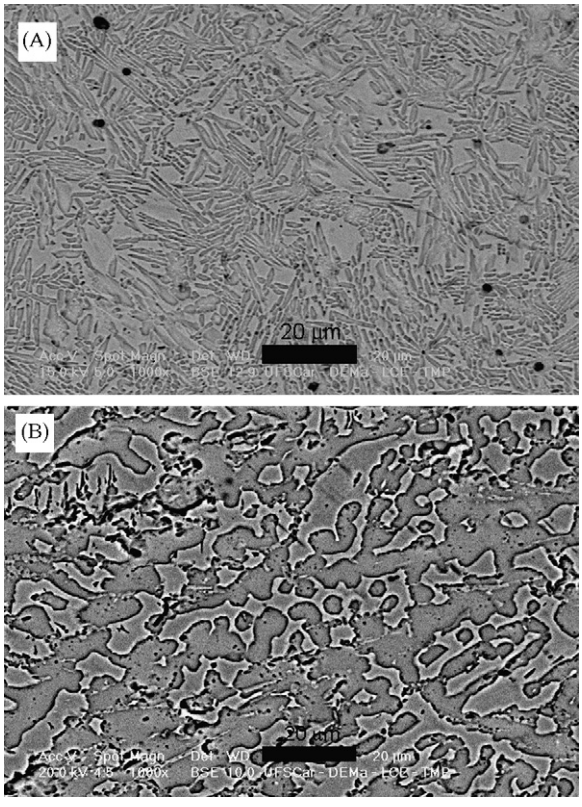

Fig. 3. (a) BSE image of the $TiMn_{1.1}V_{0.9}$ alloy and (b) BSE image of the $TiMn_{1.1}(FeV)_{0.9}$ alloy.

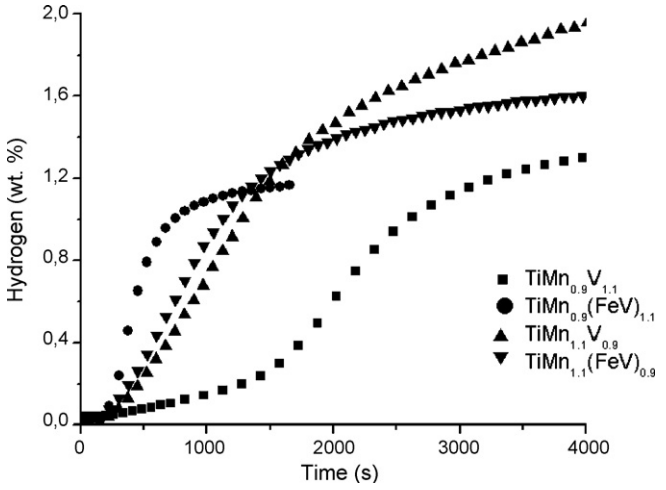

Fig. 4. Hydrogen absorption curves for the Ti–Mn–V and Ti–Mn–(FeV) alloys at 298 K.

has already a two-phase structure. This explanation agrees with Mouri and Iba [11] who reported that Ti–V–Mn BCC solid solutions with larger fractions of C14 Laves phase dispersed in the matrix showed faster hydrogenation reaction. These authors ascribed this behavior to the preferential hydrogenation of the C14 Laves phase, resulting in the expansion of its structure during hydrogenation and, consequently, creating cracks in the C14/BCC interfaces which could help the hydrogen penetration into the BCC matrix [11]. These authors also suggested the possibility of hydrogen fast diffusion through the BCC/C14 boundaries [11].

In case of the desorption curves (Fig. 5), the amount of desorbed hydrogen was not high enough to allow a careful and reliable analysis of the alloys' behavior. The limited amount of desorbed hydrogen is probably due to the low plateau pressure usually exhibited by the BCC solid solutions and also the limited vacuum achieved by our apparatus during the desorption kinetics, which presented a residual hydrogen pressure of about 33 kPa. However it is possible to observe that, under our experimental conditions, the amount of hydrogen released by the (FeV)-containing alloys was larger than that of the V-containing alloys. This feature can be related to a higher hydrogen plateau pressure of desorption for the (FeV)-

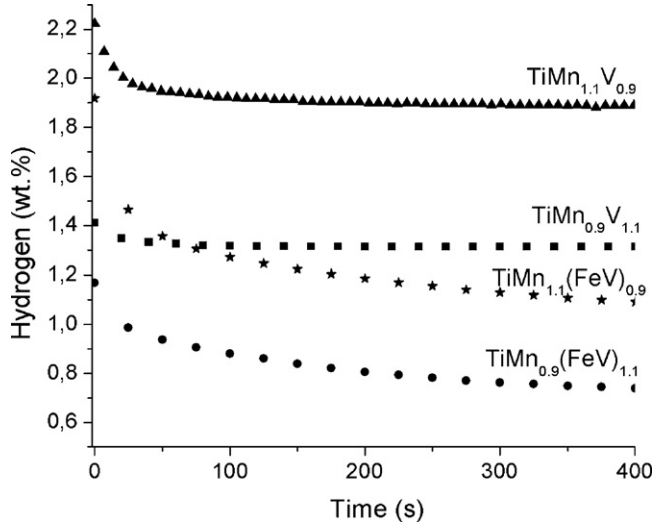

Fig. 5. Hydrogen desorption curves for the Ti–Mn–V and Ti–Mn–(FeV) alloys at 298 K.

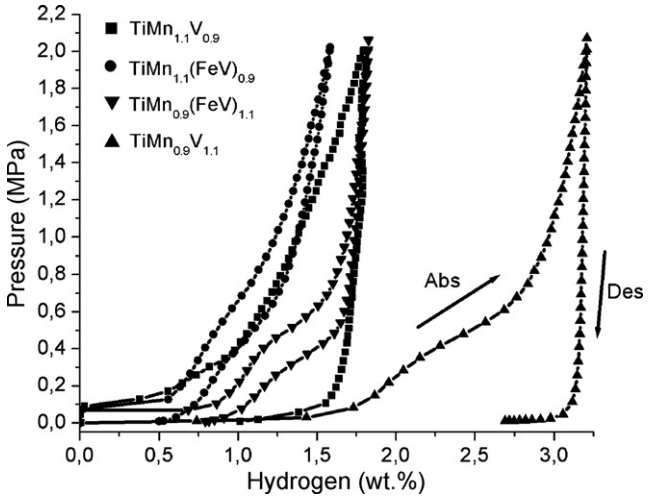

Fig. 6. PCI of the Ti–Mn–V and Ti–Mn–(FeV) alloys 353 K.

Table 2
Total and reversible hydrogen storage capacities of the Ti–Mn–V and Ti–Mn–(FeV) alloys at 353 K and maximum pressure of 2.0 MPa (uncertainties for the capacities are estimated as below 0.1 wt.%).

Alloy	Hydrogen storage capacity (wt.%)	Reversible hydrogen storage capacity (wt.%)
$TiMn_{0.9}V_{1.1}$	3.2	0.5
$TiMn_{0.9}(FeV)_{1.1}$	1.8	1.0
$TiMn_{1.1}V_{0.9}$	1.8	0.8
$TiMn_{1.1}(FeV)_{0.9}$	1.6	1.1

containing alloys, but this issue can be better analyzed through the PCI results.

Fig. 6 shows the PCI of the investigated alloys at 353 K and up to 2.0 MPa. From this figure, the plateau pressures of absorption and desorption under thermodynamic equilibrium conditions and the reversible hydrogen storage capacities (i.e., the amount of absorbed hydrogen that could be desorbed from the samples under our experimental conditions) could be evaluated. The arrow to the right-side indicates the absorption PCI while the left-side arrow indicates the desorption PCI. The largest hydrogen storage capacity was achieved for the $TiMn_{0.9}V_{1.1}$ alloy. However, the low plateau pressure of desorption hindered a large release of hydrogen. Thus, under our experimental conditions, only 0.5 wt.% of reversible hydrogen storage capacity was achieved for this alloy. The (FeV)-containing alloys presented lower total hydrogen storage capacities than those of their counterparts synthesized with pure V. Nevertheless, these (FeV)-containing alloys achieved larger reversible hydrogen storage capacities than the V-containing alloys. The reason is the increase of plateau pressures which resulted in a lower hysteresis for the (FeV)-containing alloys. A similar behavior is reported by Yu et al. [14] who investigated the hydrogen sorption properties of the $Ti_{40}Cr_{10}Mn_{18}V_{32}$ and $Ti_{40}Cr_{10}Mn_{18}V_{27}Fe_5$ alloys (in at.%) and observed that the partial replacement of Fe for V leads to a decrease in the hydrogen storage capacity, but an improvement of the reversible hydrogen storage capacity was observed.

The values of total hydrogen storage capacities and reversible storage capacities obtained from the PCI curves at 353 K (Fig. 6) are summarized in Table 2. There are differences between the values obtained for the absorbed hydrogen from the activation kinetic measurements (Fig. 4) and the PCI measurements (Fig. 6). These differences can be ascribed to the different temperatures used for the activation kinetics (298 K) and PCI (353 K) measurements. Furthermore, during the activation kinetic measurements, the samples were not fully activated and the saturation was not achieved. Thus, the values of hydrogen storage capacities obtained from PCI measurements are more reliable.

The reversible hydrogen storage capacities (Table 2) increase for the alloys with larger contents of C14 Laves phase (Fig. 1). Furthermore, Table 1 shows that the V-containing alloys have larger cell volumes than the (FeV)-containing alloys. Thus, the interstitial sites for hydrogen storage in the (FeV)-containing alloys are smaller, which could lead to an increase in the hydrogen plateau pressure.

4. Conclusions

The replacement of vanadium by commercial ferrovanadium (FeV) leads to noticeable changes in microstructure and hydrogen storage properties. Ferrovanadium-containing alloys have a higher amount of C14 Laves phase than their pure vanadium counterparts. This explains the fact that $TiMn_{0.9}(FeV)_{1.1}$ and $TiMn_{1.1}(FeV)_{0.9}$ alloys have faster activation kinetics than the alloys containing pure vanadium. Even reducing the total hydrogen storage capacity when vanadium is substituted by ferrovanadium, the reversible hydrogen storage capacity is improved because of the modification of the plateau pressures of desorption. Therefore, BCC solid solution alloys containing ferrovanadium could be considered to be a reliable low-cost system for storing hydrogen.

Acknowledgements

The authors would like to thank the financial support from the Natural Resource Canada and New Energy and Industrial Technology Development Organization (NEDO) under “Development for Safe Utilization and Infrastructure of Hydrogen”. One of the authors (S.F. Santos) would like to thank the National Council for Scientific and Technological Development (CNPq), Brazil, for the post-doctoral fellowship. The authors acknowledge the useful suggestions of Dr. S. Amira for this manuscript preparation.

References

[1] A.J. Maeland, Int. J. Hydrogen Energy 28 (2003) 821.
[2] T. Mori, H. Iba, Mater. Sci. Eng. A 329 (2002) 346.
[3] A.J. Maeland, G.G. Libowitz, J.F. Lynch, J. Less Common Met. 104 (1984) 361.
[4] S. Ono, K. Nomura, Y. Ikeda, J. Less Common Met. 72 (1980) 159.
[5] H. Iba, E. Akiba, J. Alloys Compd. 253–254 (1997) 21.
[6] E. Akiba, Curr. Opin. Solid State Mater. Sci. 4 (1999) 267.
[7] H. Taizhong, W. Zhu, X. Baojia, C. Jinzhou, Y. Xuebin, X. Naixin, L. Changwei, Y. Huimei, Sci. Technol. Adv. Mater. 4 (2003) 491.
[8] H. Taizhong, W. Zhu, C. Jinzhou, Y. Xuebin, X. Baojia, X. Naixin, Mater. Sci. Eng. A 385 (2004) 17.
[9] H. Taizhong, W. Zhu, X. Baojia, X. Naixin, Intermetallics 13 (2005) 1075.
[10] S.F. Santos, J. Huot, J. Alloys Compd. (2008), doi:10.1016/j.jallcom.2008.04.062.
[11] T. Mouri, H. Iba, Mater. Sci. Eng. A 329–331 (2002) 346.
[12] S. Challet, M. Latroche, F. Heurtaux, J. Alloys Compd. 439 (2007) 294.
[13] S.-W. Cho, E. Akiba, Y. Nakamura, H. Enoki, J. Alloys Compd. 297 (2000) 253.
[14] X.B. Yu, Z.X. Yang, S.L. Feng, Z. Wu, N.X. Xu, Int. J. Hydrogen Energy 31 (2006) 1176.